

Quantum fluctuations and unusual critical exponents in a quantum Rabi Triangle

Xiao Qin and Yu-Yu Zhang*

*Department of Physics, Chongqing Key Laboratory for strongly coupled Physics,
Chongqing University, Chongqing 401330, China*

(Dated: February 21, 2024)

Quantum fluctuations of a quantum Rabi triangle are studied using an analytical approach beyond the mean-field theory. By applying an artificial magnetic field among three cavities, time-reversal symmetry breaking is manifested through a directional transfer dynamics of photons. In contrast to previous studies, we focus on the scaling exponents of the fluctuations of the local photon number and the position variance near the critical point. By accurate calculation using Bogoliubov transformation we show that two scaling laws emerge respectively for the frustrated cavity and the remaining cavities, which are associated with the geometric frustrations. Especially, for the frustrated cavity, the scaling exponent in the chiral superradiant phase is different from that in the frustrated antiferromagnetic superradiant phase without an artificial magnetic field. The unusual scaling exponents predict distinct universality classes from the single-cavity Rabi universality. We suggest that the accurate critical exponents in few-body system is useful for identifying exotic quantum phase transition in light-matter coupling system.

I. INTRODUCTION

The interaction between light and matter has brought forth a new class of quantum many-body system in understanding of strongly correlated systems and quantum phase transition [1–4]. The effect of quantum fluctuations driving the quantum phase transitions is especially pronounced in characterizing singularity and universality classes by universal scaling laws [5–8]. A superradiant phase transition (SPT) is a remarkable phenomenon in the Dicke mode [9–13], which describes an ensemble of two-level atoms interacting with a quantized single-mode cavity. Such SPT has been found in few-body systems such as the quantum Rabi model in the limit where the atomic transition frequency in the unit of the cavity frequency tends to infinity [14–19], exhibiting the same critical exponents as the Dicke model [12–14]. A few-body system of light-atom interactions sheds new light in quantum simulation of quantum phase transitions due to its high control and tunability.

To explore intriguing quantum phases, synthetic magnetic fields are applied in atom-cavity coupling systems and photon lattices [20], chiral edge currents in atoms [21, 22], chiral ground-state currents of interacting photons [23], and fractional quantum Hall physics in the Jaynes-Cummings Hubbard lattice [24, 25]. In the presence of an artificial magnetic field, unusual superradiant phases have been found in the generalized Rabi and Dicke systems, including a chiral phase in a quantum Rabi triangle [26], chiral superradiant phases analogies to quantum magnetism in a quantum Rabi ring [27] and anomalous superradiant phases in a Dicke lattice model [28]. Such exotic SPTs exhibit unusual scaling behaviors by comparing to the conventional SPT in the Dicke model. Besides the artificial magnetic field, geometric frustration

has been proved to induce counterintuitive critical phenomena. Different critical exponents of the excitation energy have been found on the two sides of phase transitions in the Rabi triangle [27] and in the Dicke trimer [28, 29], which are associated the frustrated geometry. However, there appears to be no clear scaling exponents of quantum fluctuations near the critical value. Since there is a challenge of an accurate solution beyond a mean-field approach for the Rabi and Dicke lattice including interactions between cavities.

In this paper, we perform an analytical solution beyond the mean-field approximation for the quantum Rabi triangle with an artificial magnetic field. In contrast to previous studies, we present an analytical expression of quantum fluctuations and obtain accurate scaling exponents near the critical point. In the chiral superradiant phase (CSP), we find the fluctuation of the mean photons in the frustrated cavity diverges with an anomalous critical exponent, which is distinct from the conventional exponent of the remaining cavities. In the absence of an artificial magnetic field, the scaling exponent of the frustrated cavity in the frustrated antiferromagnetic superradiant phase (AFSP) is different from that in the CSP. Thus, the scaling behavior of quantum fluctuations in the CSP and the frustrated AFSP fall into two classes, one for the frustrated cavity and the other for the remaining cavities. Moreover, the scaling behavior below and above the transition point is different due to the frustrated local photons. In contrast, the scaling exponents are equal to each other on the two sides of the transition of the ferromagnetic superradiant phase (FSP), which are the same as that in the Dicke model.

The rest of this paper is organized as following: In Sec. II, we introduce the Hamiltonian of the quantum Rabi triangle and the dynamics of photons with an artificial magnetic field. In Sec. III, the quantum fluctuations of the mean photons and the position variance are given analytically in the normal phase below the critical value. Sec. IV gives the analytical solutions for different

* yuyuzh@cqu.edu.cn

superradiant phases and the expressions for the quantum fluctuations. Sec. V gives the scaling exponents of the quantum fluctuations and excitation energies beyond the mean-field approximation. The conclusion is given in Sec. VI.

II. HAMILTONIAN

A Rabi triangle model consists of $N = 3$ coupled cavities, and the Hamiltonian is

$$H_{\text{QRT}} = \sum_n^3 H_{R,n} + \sum_n^3 J(e^{i\theta} a_n^\dagger a_{n+1} + e^{-i\theta} a_n a_{n+1}^\dagger), \quad (1)$$

where the quantum Rabi Hamiltonian of each cavity coupled to a two-level atom is described as $H_{R,n} = \omega a_n^\dagger a_n + g(a_n^\dagger + a_n)\sigma_n^x + \frac{\Delta}{2}\sigma_n^x$. The second term of the Hamiltonian H_{QRT} describes the photons hopping between the nearest-neighbor cavities with a phase θ , which can be realized on cavities by dynamical modulating the cavity-atom coupling and photon hopping strengths [26]. An artificial vector potential $A(r)$ leads the photon hopping terms between nearby cavities n and m to become complex with the phase given by $\theta = \int_{r_n}^{r_m} A(r)dr$. The time-reversal symmetry (TRS) is artificially broken when $\theta \neq m\pi$ ($m \in \mathbb{Z}$). The effective magnetic flux is 3θ in three cavities, which form a closed loop.

To explore the effects of the artificial magnetic field we study the dynamics of photon flow in our system. At $t = 0$, a photon is prepared in the 1st cavity and the two-level atom in each cavity is in the down state, giving the initial state $|\varphi(0)\rangle = |100\rangle|\downarrow\downarrow\downarrow\rangle$. The time-evolving wave function is $|\varphi(t)\rangle = e^{-iH_{\text{QRT}}t}|\varphi_0\rangle$. The mean photon in the i -th cavity is given by $N_i = \langle\varphi(t)|a_i^\dagger a_i|\varphi(t)\rangle$.

Fig.1 shows the mean photon number evolution in each cavity dependent on θ . The photon number is initially occupied in the first cavity with $N_1 = 1$. For $\theta = 0$ in Fig.1(a), the photon transfer symmetrically from cavity 1 to cavity 2 and cavity 3 simultaneously, then back to cavity 1. There is no preferred circulation direction. Since TRS is preserved for the trivial case $\theta = 0$, the states at time t and $T - t$ satisfy $\varphi(t) = \varphi(T - t)$ with a time-evolving period T . A completely different dynamics is observed for $\theta = \pi/2$ in Fig.1(b). The photon is flowing unidirectionally, first from cavity 1, to cavity 2, to cavity 3, eventually back to cavity 1. Such chiral current direction is a signature of the breaking of TRS. Because the evolution of the state from $t = T$ backwards is different as going forwards from $t = 0$. Choosing $\theta = -\pi/2$ leads to the opposite direction of the chiral photon flow in Fig.1(c). It demonstrates that the artificial flux θ leads to the breaking of TRS, which behaves similarly to a magnetic flux.

Besides the TRS breaking induced by the artificial magnetic flux, rich superradiant phase transitions have been explored dependent on θ in the quantum Rabi triangle [26, 27]. The phase transitions occur in the limit

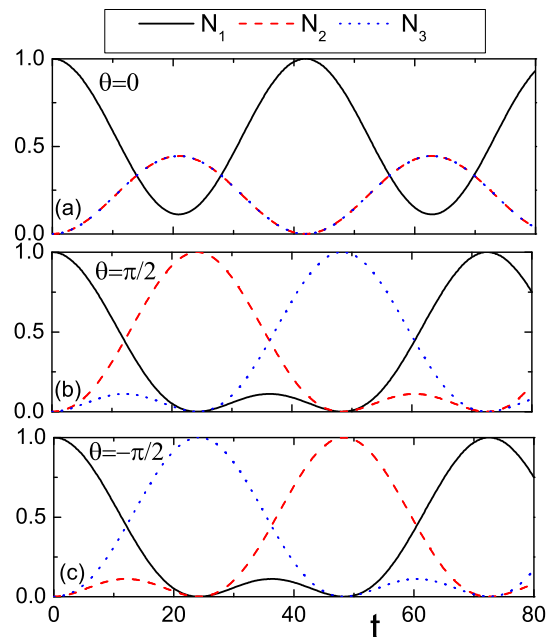


FIG. 1. Mean photon number in each cavity N_1 (black solid line), N_2 (red dashed line), N_3 (blue dotted line) as a function of time t for three values of (a) $\theta = 0$, (b) $\pi/2$ and (c) $-\pi/2$ for the scaled coupling strength $g_1 = 0.1$. In this paper we use $\Delta/\omega = 50$ and $J/\omega = 0.05$ by choosing $\omega = 1$ as the unit for frequency.

where Δ is much larger than frequency scales in the system $\Delta/\omega \rightarrow \infty$. Different from previous studies, we extract unusual critical exponents to classify the universality classes of the nontrivial phase transition by involving the geometric frustrations and the effects of the magnetic flux. In particular, quantum fluctuations are crucial to capture the singularity and scaling exponents near the critical point using an accurate solution beyond a mean-field approximation.

III. QUANTUM FLUCTUATIONS IN THE NORMAL PHASE

We perform a Schrieffer-Wolff transformation with an unitary operator $S_n = \exp[-i\sigma_n^y g_1 \sqrt{\omega/\Delta} (a_n^\dagger + a_n)]$. The lower-energy Hamiltonian is obtained by projecting H_{ICP} to the spin subspace $|\downarrow\rangle$, giving

$$H_{\text{MP}}^\downarrow = \sum_{n=1}^3 (\omega - 2\omega g_1^2) a_n^\dagger a_n - \omega g_1^2 (a_n^2 + a_n^{\dagger 2}) + J \sum_{\langle nn' \rangle} (e^{i\theta} a_n^\dagger a_{n'} + h.c.) + E_0, \quad (2)$$

where the energy constant is $E_0 = 3[-\Delta/2 - \omega g_1^2 + (\omega + J)\omega^2 g_1^2/\Delta]$.

By introducing the Fourier transformation $a_n^\dagger = \sum_q e^{inq} a_q^\dagger / \sqrt{N}$ with the quasi-momentum $q = 0, \pm 2\pi/3$, the transformed Hamiltonian is expressed as $H_{\text{ICP}}^\dagger = \sum_q \omega_q a_q^\dagger a_q - \omega g_1^2 (a_q a_{-q} + a_q^\dagger a_{-q}^\dagger) + E_0$, where $\omega_q = \omega - 2\omega g_1^2 + 2J \cos(\theta - q)$. By performing a unitary transformation $S_q = \exp[\lambda_q (a_q^\dagger a_{-q}^\dagger - a_q a_{-q})]$ with a variational squeezing parameter $\lambda_q = -\frac{1}{8} \ln \frac{\omega_q + \omega_{-q} - 4\omega g_1^2}{\omega_q + \omega_{-q} + 4\omega g_1^2}$, we derive the Hamiltonian in diagonalized form as $H_{\text{ICP}}^\dagger = \sum_q \varepsilon_q a_q^\dagger a_q + E_g$ with the ground-state energy $E_g = E_0 + \frac{1}{2} \sum_q (\varepsilon_q - \omega_q)$. The excitation spectrum is obtained as

$$\varepsilon_q^{\text{NP}} = \frac{1}{2} (\sqrt{\Omega_{+,q}^2 - 16\omega^2 g_1^4} + \Omega_{-,q}) \quad (3)$$

with the dispersion $\Omega_{\pm,q} = \omega_q \pm \omega_{-q}$. The lowest excitation energy is associated with the quasi-momentum q dependent on θ . For $\theta = 0$, the excitation energy $\varepsilon_{q=\pm 2/3}^{\text{NP}}$ with $q = \pm 2\pi/3$ becomes the lowest one, and decreases to zero for g_1 approaching g_c from below in Fig. 2(a). As θ increases, the lowest energy is determined by $q = -2\pi/3$ in Fig. 2(b). Then it changes to $\varepsilon_{q=0}^{\text{NP}}$ with $q = 0$ in Fig. 2(d). The vanishing of $\varepsilon_q^{\text{NP}} = 0$ dependent on θ and q -momentum gives the critical scaled coupling strength $g_{1c}(q) = \frac{1}{2} \sqrt{\frac{1+4J/\omega \cos q \cos \theta + 4J^2/\omega^2 \cos(\theta+q) \cos(\theta-q)}{1+2J/\omega \cos \theta \cos q}}$, which gives the phase boundary. Especially for $\theta = 0$, the critical coupling strength is $g_c(\pm 2\pi/3)$ originating from the lowest excitation energy with $q = \pm 2\pi/3$. By increasing the magnetic flux, the critical flux is given by $\theta_c = \pm \cos^{-1}[-2J/(\sqrt{8J^2 + \omega^2} + \omega)]$ by solving $g_c(\pm 2\pi/3) = g_c(0)$, which classifies phase boundary by tuning θ .

The ground-state in the NP is

$$|\varphi_{np}\rangle = \prod_q e^{\lambda_q (a_q^\dagger a_{-q}^\dagger - a_q a_{-q})} |0\rangle_q |\downarrow\rangle, \quad (4)$$

where $|\downarrow\rangle$ is the lowest state of the atom. The average photon number in the ground state can be obtained as $\langle a_q^\dagger a_q \rangle_{np} = \langle \varphi_{np} | a_q^\dagger a_q | \varphi_{np} \rangle = (\cosh 4\lambda_q - 1)/2$, which describes the quantum fluctuation of photons for g_1 approaching the critical value g_{1c} from below. The local mean photon number in the n th cavity is obtained by

$$\langle a_n^\dagger a_n \rangle_{np} = \frac{1}{N} \sum_q \langle a_q^\dagger a_q \rangle_{np} = \frac{1}{2N} \sum_q \left[\frac{\Omega_{+,q}}{2\varepsilon_q - \Omega_{-,q}} - 1 \right]. \quad (5)$$

The variance of $x_q = a_q + a_q^\dagger$ and $p_q = i(a_q^\dagger - a_q)$ are derived as $(\Delta x_q)^2 = \langle \varphi_{np} | x_q^2 | \varphi_{np} \rangle - \langle \varphi_{np} | x_q | \varphi_{np} \rangle^2 = e^{4\lambda_q}$, and $(\Delta p_q)^2 = \langle p_q^2 \rangle - \langle p_q \rangle^2 = e^{-4\lambda_q}$. The local variance of quadratures in the n th cavity is

$$(\Delta x_n)^2 = \frac{1}{N} \sum_q (\Delta x_q)^2 = \frac{\Omega_{+,q} + 4\omega g_1^2}{2\varepsilon_q - \Omega_{-,q}}, \quad (6)$$

and $(\Delta p_n)^2 = \frac{1}{N} \sum_q e^{-4\lambda_q}$.

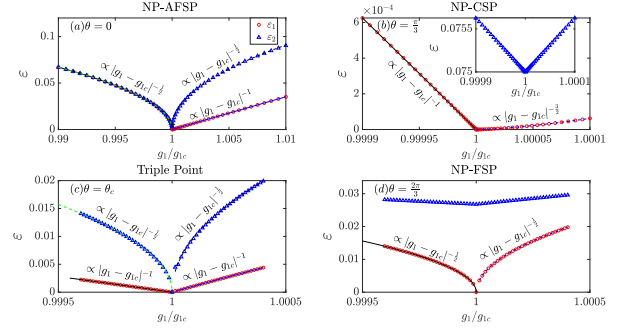


FIG. 2. The lowest and second excitation energy $\varepsilon_{1(2)}$ below and above the critical coupling strength g_{1c} for the NP-AFSP transition ($\theta = 0$)(a), the NP-CSP transition ($\theta = 0.1 < \theta_c$)(b), the triple point ($\theta = \theta_c$)(c) and the NP-FSP transition ($\theta = 1.7 > \theta_c$) (d). The parameters are $\Delta/\omega = 100$ and $J/\omega = 0.05$ by setting $\omega = 1$ as the unit for the frequency. The inset (b) shows the second excitation energy ε_2 for the NP-CSP transition, which exhibits an obvious energy gap in comparison to ε_1 .

It indicates that the singularity of the mean photon number $\langle a_n^\dagger a_n \rangle_{np}$, the variance of $(\Delta x_n)^2$ and $(\Delta p_n)^2$ is determined by the excitation energy ε_q and $\Omega_{-,q}$ in the denominator. Obviously, ε_q becomes zero at the critical value g_{1c} . It is interesting to understand the divergence from $\Omega_{-,q} = 4J \sin \theta \sin q$ dependent on q and θ . In the absence of the magnetic field with $\theta = 0$ or the momentum $q = 0$, one has $\Omega_{-,q} = 0$. It leads to the singularity of quantum fluctuations of $\langle a_n^\dagger a_n \rangle_{np}$ at the critical point in Fig. 3(a) (d) as well as $(\Delta x_n)^2$ in Fig. 4(a)(d). In contrast, for $\theta \neq 0$ and $q = \pm 2\pi/3$, it gives nonzero value of $\Omega_{-,q}$, which results in a finite value of $\langle a_n^\dagger a_n \rangle_{\text{NP}}$ and $(\Delta x_n)_{\text{NP}}^2$, respectively. There appear non-divergent fluctuations in Fig. 3(b) and Fig. 4(b) for g_1 approaching g_{1c} from below.

IV. QUANTUM FLUCTUATIONS IN THE SUPERADIANT PHASE

It is interesting to explore the quantum fluctuations and scaling exponents when g_1 approaches g_{1c} from above. As the atom-cavity coupling increases $g_1 > g_{1c}$, rich superradiant phases emerge by adjusting the flux θ [26, 27]. Since the photon population in each cavity becomes macroscopic. The bosonic operator a_n^\dagger (a_n) is expected to be shifted as $\tilde{a}_n = D^\dagger(\alpha_n) a_n D(\alpha_n) = a_n + \alpha_n$ with the complex displacement $\alpha_n = A_n + iB_n$. It is different from the mean field approximation, for which the bosonic operator a_n is replaced by its mean value $\langle a_n \rangle = \alpha_n$. The Hamiltonian in the superradiant phases

becomes

$$H_{\text{SR}}^\dagger = \sum_{n=1}^3 \omega \tilde{a}_n^\dagger a_n - \frac{\Delta_n}{2} \tau_n^z + \lambda_n (\tilde{a}_n^\dagger + \tilde{a}_n) \tau_n^x + J a_n^\dagger (e^{i\theta} \tilde{a}_{n+1} + e^{-i\theta} \tilde{a}_{n-1}) + V_{\text{off}} + E_0, \quad (7)$$

where the transformed Pauli matrix is $\tau_n^z = \Delta/\Delta_n \sigma_n^z + 4gA_n/\Delta_n \sigma_n^x$ with the renormalized parameter $\Delta_n = \sqrt{\Delta^2 + 16g^2 A_n^2}$, and the effective coupling strength is $\lambda_n = g\Delta/\Delta_n$. The off-diagonal term is expressed as $V_{\text{off}} = \sum_n \omega(\alpha_n a_i^\dagger + \alpha_n^* a_n) + g(a_n^\dagger + a_n) \sin(2\gamma_n) \sigma_n^z + J[a_n^\dagger(e^{i\theta} \alpha_{n+1} + e^{-i\theta} \alpha_{n-1}) + h.c.]$. By eliminating V_{off} term, we obtain equations explicitly

$$0 = \omega A_n - g \sin(2\gamma_n) + J[(A_{n+1} + A_{n-1}) \cos \theta + (B_{n-1} - B_{n+1}) \sin \theta] = 0, \quad (8)$$

and

$$0 = \omega B_n + J[\cos \theta (B_{n+1} + B_{n-1}) + \sin \theta (A_{n+1} - A_{n-1})]. \quad (9)$$

α_n can be accurately obtained by solving above equations. The lowest-energy Hamiltonian is obtained by projecting to the spin subspace $|\downarrow\rangle$, giving

$$H_{\text{eff}}^\dagger = \sum_{n=1}^3 \omega a_n^\dagger a_n - \frac{\lambda_n^2}{\Delta_n} (a_n^\dagger + a_n)^2 + J a_n^\dagger (e^{i\theta} a_{n+1} + e^{-i\theta} a_{n-1}) + E_g. \quad (10)$$

where the ground-state energy is $E_g = \sum_n \omega \alpha_n^* \alpha_n + J \sum_n \alpha_n^* (e^{i\theta} \alpha_{n+1} + e^{-i\theta} \alpha_{n-1}) - \Delta_n/2$.

Superradiant phases can be characterized by the order parameter α_n . Firstly, for $\theta = 0$ and $g_1 > g_{1c}^{\text{AFSP}} (\pm 2\pi/3)$, the system is in the frustrated AFSP. α_n is real with opposite signs for the neighboring cavities. It corresponds to an AFSP with antiferromagnetic order. Moreover, geometric frustration in three cavities yields site-dependent α_n , so-called frustrated AFSP. The ground state breaks the C_3 symmetry. Secondly, for $0 < \theta < \theta_c$, the system enters the CSP regime above the critical coupling strength $g_c^{\text{CSP}} (-2\pi/3)$ [26]. α_n is complex and n dependent, which is different from that in the AFSP. For $\theta_c < \theta \leq \pi$ the displacement in each cavity α_n is real and is independent of n , which gives $\alpha_n = \pm \sqrt{16g^4/(\omega + 2J\cos\theta)^2 - \Delta^2}/(4g)$. It forms a ferromagnetic order with the same displacement of the neighboring cavities for $g_1 > g_{1c}^{\text{FSP}} (q = 0)$. It corresponds to the FSP.

The Hamiltonian in Eq. (10) is bilinear in the creation and annihilation operators a_i^\dagger and a_i , which captures the quantum fluctuations especially near the critical coupling strength g_c . It can be diagonalized by the bosonic Bogoliubov transformation. By using the denotation $\alpha = \{a_1, a_2, a_3, a_1^\dagger, a_2^\dagger, a_3^\dagger\}$, the Hamiltonian in Eq. (10) can be written in matrix form as $H_{\text{eff}}^\dagger = \alpha M \alpha^\dagger - 3(\omega - \lambda_n^2/\Delta_n)/2$, where a transformed matrix M is

$$M = \begin{pmatrix} \omega/2 - \lambda_1^2/\Delta_1 & J e^{-i\theta}/2 & J e^{i\theta}/2 & -\lambda_1^2/\Delta_1 & 0 & 0 \\ J e^{i\theta}/2 & \omega/2 - \lambda_2^2/\Delta_2 & J e^{-i\theta}/2 & 0 & -\lambda_2^2/\Delta_2 & 0 \\ J e^{-i\theta}/2 & J e^{i\theta}/2 & \omega/2 - \lambda_3^2/\Delta_3 & 0 & 0 & -\lambda_3^2/\Delta_3 \\ -\lambda_1^2/\Delta_1 & 0 & 0 & \omega/2 - \lambda_1^2/\Delta_1 & J e^{i\theta}/2 & J e^{-i\theta}/2 \\ 0 & -\lambda_2^2/\Delta_2 & 0 & J e^{-i\theta}/2 & \omega/2 - \lambda_2^2/\Delta_2 & J e^{i\theta}/2 \\ 0 & 0 & -\lambda_3^2/\Delta_3 & J e^{i\theta}/2 & J e^{-i\theta}/2 & \omega/2 - \lambda_3^2/\Delta_3 \end{pmatrix}. \quad (11)$$

We perform a Bogoliubov's transformation to give bosonic operators $\beta = \{b_1^\dagger, b_2^\dagger, b_3^\dagger, b_1, b_2, b_3\}$ as a linear combination of $\alpha = \{a_1^\dagger, a_2^\dagger, a_3^\dagger, a_1, a_2, a_3\}$, which satisfies $\alpha^\dagger = T\beta^\dagger$ with a paraunitary matrix T rather than a unitary matrix. To ensure the bosonic commutation relation, the paraunitary matrix T satisfies the relations of $T^\dagger \Lambda T = T \Lambda T^\dagger = \Lambda$, where $\Lambda = \begin{pmatrix} I_{3 \times 3} & 0 \\ 0 & -I_{3 \times 3} \end{pmatrix}$ with $I_{3 \times 3}$ being the identity matrix of order 3. Substituting for α and α^\dagger in terms of β^\dagger and β , one obtains the diagonalized form as

$$H_{\text{eff}}^\dagger = \beta T^\dagger M T \beta^\dagger = 2 \sum_{k=1}^3 \varepsilon_k b_k^\dagger b_k + \frac{\varepsilon_k - \omega}{2}, \quad (12)$$

where ε_k is the corresponding eigenvalue for each excitation mode. The eigenvalues $\pm \varepsilon_n$ are obtained by di-

agonalizing the matrix ΛM as $T^{-1} \Lambda M T = \Lambda \varepsilon$. The corresponding eigenvector gives the k -th column vector of the paraunitary matrix as $T_k = [T_{1k}, T_{2k}, \dots, T_{6k}]^T$.

The ground state in the superradiant phases is the vacuum state

$$|\varphi_{\text{SR}}\rangle = |0\rangle_{b_1} |0\rangle_{b_2} |0\rangle_{b_3}, \quad (13)$$

where $|0\rangle_{b_n}$ satisfies $b_n |0\rangle_{b_n} = 0$. Note that the operator b_n corresponds to the original operator a_n with the displacement transformation $D(\alpha)$ and the transformation $\alpha^\dagger = T\beta^\dagger$. One obtains $a_n = \sum_{i=1}^3 T_{n,i} b_i + T_{n,i+3} b_i^\dagger + \alpha_n$. The local photon number in the n th cavity of the ground state $|\varphi_{\text{SR}}\rangle$ is derived explicitly as

$$\langle a_n^\dagger a_n \rangle = |T_{n4}|^2 + |T_{n5}|^2 + |T_{n6}|^2 + |\alpha_n|^2. \quad (14)$$

The variance of x_n and p_n are

$$(\Delta x_n)^2 = |T_{n1} + T_{n4}^*|^2 + |T_{n2} + T_{n5}^*|^2 + |T_{n3} + T_{n6}^*|^2, \quad (15)$$

and $(\Delta p_n)^2 = |T_{n4}^* - T_{n1}|^2 + |T_{n5}^* - T_{n2}|^2 + |T_{n6}^* - T_{n3}|^2$, which are derived in detail in Appendix. Thus the quantum fluctuations of $(\Delta x_n)^2$ and $\langle a_n^\dagger a_n \rangle$ are obtained beyond the mean-field approximation. We calculate the scaling behaviors of the critical fluctuations in the vicinity of the critical value g_c in the following.

V. UNUSUAL CRITICAL EXPONENTS

Our major interests are the scaling exponents of the quantum fluctuations as g_1 approaches g_c for the second-order phase transitions from the NP to different super-radiant phases. Generally, the energy gap which is measured by the lowest excitation energy ε_1 vanishes as g_1 approaches g_{1c}

$$\varepsilon_1 \propto |g_1 - g_{1c}|^\gamma. \quad (16)$$

Here the critical exponent $\gamma = z\nu$ is usually universal [6], which is independent of most of the parameters of the Hamiltonian. In addition to the vanishing energy gap, a length scale which measures the correlations at the longest distances becomes diverge at the critical value. The variance of position quadrature plays an analogous role of the diverging length scale, which diverges as

$$\Delta x \propto |g_1 - g_{1c}|^{-\nu} \quad (17)$$

with a critical exponent ν . It leads to the dynamical critical exponent $z = \gamma/\nu$. Meanwhile, the fluctuations of the local mean photons near the critical value diverges as

$$\langle a_n^\dagger a_n \rangle \propto |g_1 - g_{1c}|^{-\beta}, \quad (18)$$

where β is a critical exponent. Using the Bogoliubov's diagonalization method, we calculate the scaling exponents of the lowest excitation energy ε_1 , the fluctuation of position variance $(\Delta x)^2$ in Eq.(15) and photons $\langle a_n^\dagger a_n \rangle$ in Eq.(14).

For the second-order phase transition between the NP and the frustrated AFSP with $\theta = 0$, Fig. 2(a) shows ε_1 closing the gap at g_{1c} with the exponent $1/2$ for $g_1 < g_{1c}$. In contrast, two excitation energies ε_1 and ε_2 vanish at the critical point for $g_1 > g_{1c}$

$$\varepsilon_{1,\text{AFSP}} \propto |g_1 - g_{1c}|^{-1}, \varepsilon_{2,\text{AFSP}} \propto |g_1 - g_{1c}|^{-1/2}. \quad (19)$$

It exhibits two different exponents γ_+ (γ_-) at the two sides of phase transition for $g_1 > g_{1c}$ ($g < g_{1c}$), which is distinguished from the conventional second-order phase transitions. The universal exponent $\gamma_- = 1/2$ is the same as a mean-field exponent of the Rabi model [14]. While two different exponents $\gamma_+ = 1/2$ and $\gamma_+ = 1$ in Eq.(19) appear for $g_1 > g_{1c}$, for which the latter is the unconventional scaling exponent beyond the mean-field one. The

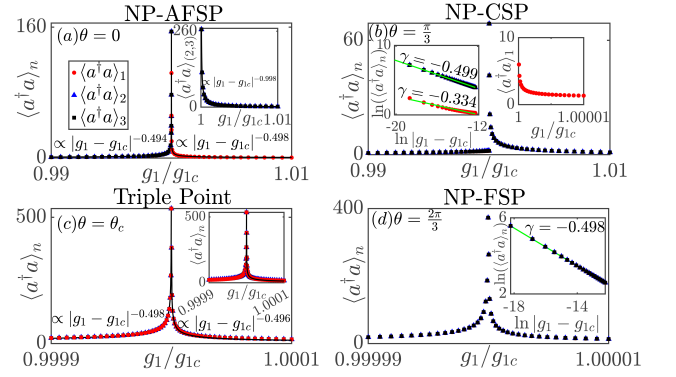


FIG. 3. Quantum fluctuations of the local mean photons for the n th cavity $a_n^\dagger a_n$ as a function of g_1/g_{1c} for the NP-AFSP transition ($\theta = 0$) (a), the NP-CSP transition ($\theta = 0.1 < \theta_c$) (b), the triple point ($\theta = \theta_c$) (c), and the NP-FSP transition ($\theta = 1.7 > \theta_c$) (d). The inset (a) shows the scaling behavior of $a_{2(3)}^\dagger a_{2(3)}$. The right side of the inset (b) shows the behavior of $a_1^\dagger a_1$, and the left side shows the scaling exponents. The inset (c) shows the scaling results by the solution in the CSP, which is same as one obtained by the solution in the FSP. The inset (d) shows the exponent .

distinct scaling behavior are consistent with results in the Dicke trimer [29]. Meanwhile, Fig. 3(a) shows the fluctuations of the mean photons in each cavity diverging with the same exponent $\beta_- = 1/2$ for $g_1 < g_{1c}$. However, for $g_1 > g_{1c}$, the photon number diverges locally dependent on n , which is associated with the frustrated geometry. $\langle a_n^\dagger a_n \rangle$ for the n th cavity exhibits different scaling law as

$$\begin{aligned} \langle a_1^\dagger a_1 \rangle_{\text{AFSP}} &\propto |g_1 - g_{1c}|^{-1}, \\ \langle a_{2(3)}^\dagger a_{2(3)} \rangle_{\text{AFSP}} &\propto |g_1 - g_{1c}|^{-1/2}. \end{aligned} \quad (20)$$

The scaling of the frustrated cavity ($n = 1$) yields an unusual exponent $\beta = 1$, while the remaining cavities ($n = 2, 3$) diverges with the same exponent $\beta = 1/2$ as that in the Rabi model, respectively. The similar n -dependent fluctuation of $(\Delta x_n)^2$ is shown in Fig. 4(a). The scaling exponent of Δx_n of each cavity below the critical value g_{1c} is the same $\nu_- = 1/4$ for $g_1 < g_{1c}$. By contrast, for $g_1 > g_{1c}$ the fluctuation diverges respectively

$$\begin{aligned} (\Delta x_1)^2_{\text{AFSP}} &\propto |g_1 - g_{1c}|^{-1}, \\ (\Delta x_{2(3)})^2_{\text{AFSP}} &\propto |g_1 - g_{1c}|^{-1/2}. \end{aligned} \quad (21)$$

The scaling exponents are extracted $\nu_+ = 1/2$ for the frustrated cavity and $\nu_+ = 1/4$ for the remaining cavities.

For the NP-CSP transition with $0 < \theta < \theta_c$, the unusual mode ε_1 closes the gap for g_1 approaching g_{1c} from below or above in Fig. 2(b). It behaves as

$$\varepsilon_{1,\text{NP}} \propto |g_1 - g_{1c}|^{-1}, \varepsilon_{1,\text{CSP}} \propto |g_1 - g_{1c}|^{-3/2}. \quad (22)$$

It gives two unconventional exponents $\gamma_- = 1$ and $\gamma_+ = 3/2$ below and above g_{1c} , which are different from results

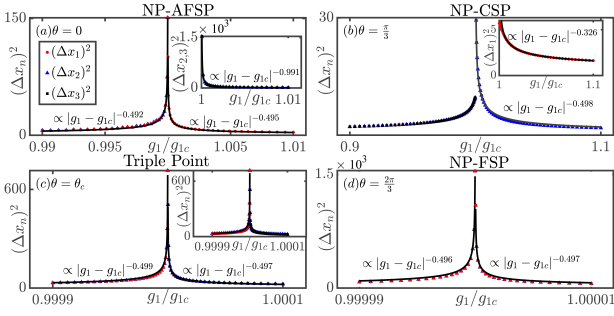


FIG. 4. Quantum fluctuation of the variance of position for the n th cavity $(\Delta x_n)^2$ as a function of g_1/g_{1c} for the NP-AFSP transition ($\theta = 0$) (a), the NP-CSP transition ($\theta = 0.1 < \theta_c$) (b), the triple point ($\theta = \theta_c$) (c), and the NP-FSP transition ($\theta = 1.7 > \theta_c$) (d). The inset (a) shows the scaling behavior of $(\Delta x_{2(3)})^2$. The inset (b) shows the fluctuations of the first frustrated cavity $(\Delta x_{1(3)})^2$ above g_{1c} . The inset (c) shows the scaling results by the solution in the CSP, which is same as one obtained by the solution in the FSP.

in the NP-AFSP transition. In contrast to the divergence at g_{1c} , one observes a finite value of $\langle a_n^\dagger a_n \rangle_{\text{NP}}$ and $(\Delta x_n)_{\text{NP}}$ when g_1 approaches g_{1c} from below in Fig. 3 (b) and Fig. 4(b). The results are consistent with the analysis from Eq.(5) and (6), for which the denominator is nonzero at the critical point for $q = \pm 2\pi/3$. For $g_1 > g_{1c}$, Fig. 3(b) shows n -dependent scaling behaviors of the local photon number

$$\begin{aligned} \langle a_1^\dagger a_1 \rangle_{\text{CSP}} &\propto |g_1 - g_{1c}|^{-1/3}, \\ \langle a_{2(3)}^\dagger a_{2(3)} \rangle_{\text{CSP}} &\propto |g_1 - g_{1c}|^{-1/2}. \end{aligned} \quad (23)$$

$\langle a_1^\dagger a_1 \rangle$ of the frustrated cavity diverges with the exponents $1/3$, which is different from that in the AFSP. The anomalous exponent $\nu_+ = 1/3$ of the frustrated cavity is more accurate by comparing to that in the Dicke lattice [28]. Meanwhile, Fig. 4(b) shows the fluctuation of the position variance of the n th cavity, which diverges as

$$\begin{aligned} (\Delta x_{1(3)})_{\text{CSP}}^2 &\propto |g_1 - g_{1c}|^{-1/3}, \\ (\Delta x_{2(3)})_{\text{CSP}}^2 &\propto |g_1 - g_{1c}|^{-1/2}. \end{aligned} \quad (24)$$

The unusual exponent $\nu_+ = 1/6$ of the frustrated cavity is also different from $\nu_+ = 1/2$ in the AFSP transition. Since the CSR phase transition is associated with both of the geometry frustration and the artificial magnetic field. It exhibits distinct exponents of the frustrated cavity by comparing to the frustrated AFSP transition with $\theta = 0$. They belong to different universality classes of phase transitions, which are distinguished from the conventional superradiant phase transition in the Dicke and Rabi model.

At the triple point θ_c , the CSR phase, FSP and NP coexist. There appear two excitation modes closing the gaps at g_{1c} . Fig. 2(c) show two different power laws behaviors

$$\varepsilon_{1,\text{TP}} \propto |g_1 - g_{1c}|^{-1}, \varepsilon_{2,\text{TP}} \propto |g_1 - g_{1c}|^{-1/2}. \quad (25)$$

TABLE I. Scaling exponents γ_\pm of the excitation energy ε_n , ν_\pm and β_\pm for quantum fluctuations of the Δx_n and $\langle a_n^\dagger a_n \rangle$ on two sides of phase transitions of the NP-AFSP ($\theta = 0$), NP-CSP ($\theta < \theta_c$), and NP-FSP ($\theta > \theta_c$) as well as the triple point (TP) ($\theta = \theta_c$).

	γ_-	γ_+	ν_-	ν_+	β_-	β_+
NP-AFSP	1/2	1, 1/2	1/4	1/2, 1/4	1/2	1, 1/2
NP-CSP	1	3/2	/	1/6, 1/4	/	1/3, 1/2
TP	1, 1/2	1, 1/2	1/4	1/4	1/2	1/2
NP-FSP	1/2	1/2	1/4	1/4	1/2	1/2

We obtain exponents $\gamma_\pm = 1$ and $\gamma_\pm = 1/2$. It is a signature of the coexistence of both CSP and FSP. And scaling exponents are the same at the two sides of the TP. We calculate the the fluctuation of $\langle a_n^\dagger a_n \rangle$ by the analytical solutions in the FSP phase in Fig. 3(c), which behaves the same as the solution in the CSR in the inset. Fig. 4(c) show the scaling laws of $(\Delta x_n)_{\text{TP}}^2$. We obtain the scaling behaviors near the critical point

$$\langle a_n^\dagger a_n \rangle_{\text{TP}} \propto |g_1 - g_{1c}|^{-1/2}, (\Delta x_n)_{\text{TP}}^2 \propto |g_1 - g_{1c}|^{-1/2}. \quad (26)$$

Thus, we obtain the scaling exponents $\beta = 1/2$ and $\nu = 1/4$ for the fluctuations of photon number and the position variance at the triple point, respectively.

For the NP-FSP transition, the scaling laws holds with the same value of the exponent γ both for $g_1 > g_{1c}$ and $g < g_{1c}$. The exponent of the excitation energy at the two sides of the phase transition are the same $\gamma_+ = \gamma_- = 1/2$ in Fig. 2(d). And the mean photons of the n th cavity diverges with the same exponent $\beta_\pm = 1/2$ in Fig. 3(d). Fig. 3(d) show the exponent $\nu_\pm = 1/4$ for the fluctuation of the position variance.

Various critical exponents for g_1 approaching g_{1c} from below and above are listed in Table I for different superradiant phase transitions. Scaling exponents below and above g_{1c} are different for the NP-AFSP and NP-CSP transition, while are the same for the NP-FSP transition. For the special frustrated cavity, the unusual critical exponent of the photon fluctuations are $\beta_+ = 1$ and $\beta_+ = 1/3$ for the NP-AFSP and NP-CSP transition, respectively. Meanwhile, the anomalous exponents of the fluctuations of the position variance are $\nu_+ = 1/2$ and $\nu_+ = 1/6$. They are distinguished from the exponents of the remaining cavities with $\beta_+ = 1/2$ and $\nu_+ = 1/4$, which are the same exponents as that in the conventional quantum Rabi model. It demonstrates that the artificial magnetic field and geometric fluctuations yield unusual exponents, which predict nontrivial universality classes of superradiant phase transitions.

VI. CONCLUSION

we have demonstrated quantum fluctuations and scaling behaviors by using an analytical approach and a Bogoliubov transformation in the Rabi triangle with an artificial magnetic field. The time-reversal symmetry breaking is observed from the photon population dynamics, exhibiting the effects of an artificial magnetic field. Due to the frustrations of the triangular geometry, there emerges two scaling laws, one for the frustrated cavity with an unusual exponent and the other for the remaining cavities with the same exponent as the conventional Dicke model. For the fluctuations of the local photon number and the position variance, the scaling exponents of the frustrated cavity are $\beta_+ = 1/3$ and $\nu_+ = 1/6$ for the CSP transition, which are distinct from $\beta_+ = 1$ and $\nu_+ = 1/2$ for the frustrated AFSP transition without an artificial magnetic flux. Moreover, the scaling exponents are different on two sides of the phase transition from the NP to the CSP and AFSP. The unconventional critical exponents predict different universality classes beyond the conventional single-cavity Rabi model. Therefore, our work paves a way for exploring unconventional phase transitions in the few-body light-matter interacting system.

ACKNOWLEDGMENTS

The authors thank Qing-Hu Chen and Xiang-You Chen for useful discussions. This work was supported by NSFC under Grant No.12075040 and No. 12347101.

Appendix A: Derivations of quantum fluctuations

In the superradiant phase, the operator a_n is shifted as $a_n + \alpha_n$. Using the Bogoliubov's diagonalization method, the ground state of the photon part is obtained as $|\varphi_{\text{SR}}\rangle = |0\rangle_{b_1}|0\rangle_{b_2}|0\rangle_{b_3}$ with $b_n|0\rangle_{b_n} = 0$. With the transformation $D(\alpha)$ and the transformation $\alpha^\dagger = T\beta^\dagger$, the operator a becomes $a_n = \sum_{i=1}^3 T_{n,i}b_i + T_{n,i+3}b_i^\dagger + \alpha_n$. The expected

value of $x_n = (a_n + a_n^\dagger)$ is given by

$$\begin{aligned} \langle x_n \rangle &= b_n \langle 0 | (a_n + a_n^\dagger) | 0 \rangle_{b_n} = \alpha_n + \alpha_n^* \\ &+ b_n \langle 0 | \sum_{i=1}^3 T_{n,i}b_i + T_{n,i+3}b_i^\dagger + T_{n,i}^*b_i^\dagger + T_{n,i+3}^*b_i | 0 \rangle_{b_n} \\ &= \alpha_n^* + \alpha_n. \end{aligned} \quad (\text{A1})$$

Then we derive the mean value of x_n^2 as

$$\begin{aligned} \langle x_n^2 \rangle &= b_n \langle 0 | (a_n + a_n^\dagger + \alpha_n^* + \alpha_n)^2 | 0 \rangle_{b_n} \\ &= \langle (a_n + a_n^\dagger)^2 + (\alpha_n^* + \alpha_n)(a_n + a_n^\dagger) \rangle + (\alpha_n^* + \alpha_n)^2 \\ &= \langle \varphi_{\text{SR}} | [(T_{n1} + T_{n4}^*)b_1 + (T_{n2} + T_{n5}^*)b_2 \\ &\quad + (T_{n3} + T_{n6}^*)b_3 + h.c.]^2 | \varphi_{\text{SR}} \rangle + (\alpha_n^* + \alpha_n)^2 \\ &= |T_{n1} + T_{n4}^*|^2 + |T_{n2} + T_{n5}^*|^2 \\ &\quad + |T_{n3} + T_{n6}^*|^2 + (\alpha_n^* + \alpha_n)^2. \end{aligned}$$

The expected value of the variance of Δx_n is obtained as

$$\begin{aligned} (\Delta x_n)^2 &= \langle x_n^2 \rangle - \langle x_n \rangle^2 \\ &= |T_{n1} + T_{n4}^*|^2 + |T_{n2} + T_{n5}^*|^2 + |T_{n3} + T_{n6}^*|^2. \end{aligned} \quad (\text{A2})$$

Additionally, the expected value of the momentum quadrature $p_n = i(a_n^\dagger - a_n)$ is

$$\langle p_n \rangle = b_n \langle 0 | i(a_n^\dagger - a_n + \alpha_n^* - \alpha_n) | 0 \rangle_{b_n} = i(\alpha_n^* - \alpha_n). \quad (\text{A3})$$

The expected value of p_n^2 is derived as

$$\begin{aligned} \langle p_n^2 \rangle &= b_n \langle 0 | - (a_n^\dagger - a_n + \alpha_n^* - \alpha_n)^2 | 0 \rangle_{b_n} \\ &= -\langle (a_n^\dagger - a_n)^2 + (\alpha_n^* - \alpha_n)(a_n^\dagger - a_n) \rangle - (\alpha_n^* - \alpha_n)^2 \\ &= -\langle [(T_{n4}^* - T_{n1})b_1 + (T_{n5}^* - T_{n2})b_2 + (T_{n6}^* - T_{n3})b_3 \\ &\quad - (T_{n4} - T_{n1}^*)b_1^\dagger - (T_{n5} - T_{n2}^*)b_2^\dagger - (T_{n6} - T_{n3}^*)b_3^\dagger]^2 \rangle \\ &\quad - (\alpha_n^* - \alpha_n)^2 \\ &= |T_{n4}^* - T_{n1}|^2 + |T_{n5}^* - T_{n2}|^2 + |T_{n6}^* - T_{n3}|^2 \\ &\quad - (\alpha_n^* - \alpha_n)^2. \end{aligned} \quad (\text{A4})$$

Then one obtains the variance of Δp_n

$$\begin{aligned} (\Delta p_n)^2 &= \langle p_n^2 \rangle - \langle p_n \rangle^2 \\ &= |T_{n4}^* - T_{n1}|^2 + |T_{n5}^* - T_{n2}|^2 + |T_{n6}^* - T_{n3}|^2. \end{aligned} \quad (\text{A5})$$

-
- [1] M. J. Hartmann, F. G. S. L. Brandão, and M. B. Plenio, *Nature Physics* **2**, 849 (2006).
[2] D. Rossini and R. Fazio, *Phys. Rev. Lett.* **99**, 186401 (2007).
[3] I. Carusotto, D. Gerace, H. E. Türeci, S. De Liberato, C. Ciuti, and A. Imamoglu, *Phys. Rev. Lett.* **103**, 033601 (2009).
[4] M. Schiró, M. Bordyuh, B. Öztóp, and H. E. Türeci, *Phys. Rev. Lett.* **109**, 053601 (2012).
[5] M. Vojta, *Rep. Prog. Phys.* **66**, 2069 (2003).
[6] S. Sachdev, *Quantum Phase Transitions*, 2nd ed. (Cambridge University Press, Cambridge, 2011).
[7] J. Cardy, (1996).
[8] S. L. Sondhi, S. M. Girvin, J. P. Carini, and D. Shahar, *Rev. Mod. Phys.* **69**, 315 (1997).
[9] R. H. Dicke, *Phys. Rev.* **93**, 99 (1954).
[10] C. Emary and T. Brandes, *Phys. Rev. E* **67**, 066203 (2003).

- [11] K. Baumann, R. Mottl, F. Brennecke, and T. Esslinger, Phys. Rev. Lett. **107**, 140402 (2011).
- [12] Q.-H. Chen, Y.-Y. Zhang, T. Liu, and K.-L. Wang, Phys. Rev. A **78**, 051801 (2008).
- [13] T. Liu, Y.-Y. Zhang, Q.-H. Chen, and K.-L. Wang, Phys. Rev. A **80**, 023810 (2009).
- [14] M.-J. Hwang, R. Puebla, and M. B. Plenio, Phys. Rev. Lett. **115**, 180404 (2015).
- [15] S. Ashhab, Phys. Rev. A **87**, 013826 (2013).
- [16] M. Liu, S. Chesi, Z.-J. Ying, X. Chen, H.-G. Luo, and H.-Q. Lin, Phys. Rev. Lett. **119**, 220601 (2017).
- [17] X.-Y. Chen, Y.-Y. Zhang, L. Fu, and H. Zheng, Phys. Rev. A **101**, 033827 (2020).
- [18] X. Chen, Z. Wu, M. Jiang, X.-Y. Lü, X. Peng, and J. Du, Nat. Commun. **12**, 1 (2021).
- [19] M. L. Cai and et al., Nat. Commun. **12**, 1126 (2021).
- [20] J. Dalibard, F. Gerbier, G. Juzeliūnas, and P. Öhberg, Rev. Mod. Phys. **83**, 1523 (2011).
- [21] H. Cai, J. Liu, J. Wu, Y. He, S.-Y. Zhu, J.-X. Zhang, and D.-W. Wang, Phys. Rev. Lett. **122**, 023601 (2019).
- [22] Y. Li, H. Cai, D.-w. Wang, L. Li, J. Yuan, and W. Li, Phys. Rev. Lett. **124**, 140401 (2020).
- [23] P. Roushan, C. Neill, A. Megrant, Y. Chen, R. Babush, R. Barends, B. Campbell, Z. Chen, B. Chiaro, A. Dunsworth, *et al.*, Nat. Phys. **13**, 146 (2017).
- [24] A. L. Hayward, A. M. Martin, and A. D. Greentree, Phys. Rev. Lett. **108**, 223602 (2012).
- [25] A. L. Hayward and A. M. Martin, Phys. Rev. A **93**, 023828 (2016).
- [26] Y.-Y. Zhang, Z.-X. Hu, L. Fu, H.-G. Luo, H. Pu, and X.-F. Zhang, Phys. Rev. Lett. **127**, 063602 (2021).
- [27] D. Fallas Padilla, H. Pu, G.-J. Cheng, and Y.-Y. Zhang, Phys. Rev. Lett. **129**, 183602 (2022).
- [28] J. Zhao and M.-J. Hwang, Phys. Rev. Res. **5**, L042016 (2023).
- [29] J. Zhao and M.-J. Hwang, Phys. Rev. Lett. **128**, 163601 (2022).